

Discovery of cyclopentane- and cyclohexane-*trans*-1,3-diamines as potent melanin-concentrating hormone receptor 1 antagonists

Fabrizio Giordanetto,^{a,*} Olle Karlsson,^b Jan Lindberg,^b Lars-Olof Larsson,^c
Anna Linusson,^d Emma Evertsson,^a David G. A. Morgan^e and Tord Inghardt^{b,*}

^aLead Generation, Computational Chemistry, AstraZeneca R&D Mölndal, SE-431 83 Mölndal, Sweden

^bMedicinal Chemistry, AstraZeneca R&D Mölndal, SE-431 83 Mölndal, Sweden

^cDMPK&BAC, AstraZeneca R&D Mölndal, SE-431 83 Mölndal, Sweden

^dOrganic Chemistry, Department of Chemistry, Umeå University, SE-901 78 Umeå, Sweden

^eCVGI Bioscience, AstraZeneca R&D Alderley Park, Macclesfield, Cheshire SK10 4TG, UK

Received 27 March 2007; revised 6 May 2007; accepted 11 May 2007

Available online 17 May 2007

Abstract—We herein report the optimization of cyclopentane- and cyclohexane-1,3-diamine derivatives as novel and potent MCH-R1 antagonists. Structural modifications of the 2-amino-quinoline and thiophene moieties found in the initial lead compound served to improve its metabolic stability profile and MCH-R1 affinity, and revealed unprecedented SAR when compared to other 2-amino-quinoline-containing MCH-R1 antagonists.

© 2007 Elsevier Ltd. All rights reserved.

Melanin-concentrating hormone (MCH) is a cyclic neuropeptide mainly expressed in the lateral hypothalamic area and the zona incerta region of the brain.^{1,2} MCH is known to play a key role in the fine regulation of feeding behavior and energy homeostasis.^{3,4} Particularly, a single administration of MCH in rats induces food-intake,⁵ while chronic intracerebroventricular (ICV) infusion substantially increases body-weight.⁶ Interestingly, mice overexpressing the MCH gene appear to be hyperphagic and prone to obesity, and display insulin-resistance,⁷ whereas transgenic MCH-R1 knockout mice are lean, resistant to diet-induced obesity, and show hyperactivity.⁸ Consequently, selective MCH-R1 antagonism could provide a viable treatment for obesity. As a result of such pharmacological validation, the search for MCH-R1 antagonists is a highly active field of medicinal chemistry research and several MCH-R1 antagonists have appeared in the literature, as exemplified by **1–6** in Figure 1.⁹ We describe herein the discovery of cyclopentane- and cyclohexane-1,3-diamines as novel and highly potent MCH-R1 antagonists.

High-throughput screening (HTS) of the AstraZeneca compound collection in a MCH-R1 binding assay and the subsequent hit-to-lead efforts resulted in the identification of **7** as a very potent MCH-R1 antagonist with a IC_{50} value of 15 nM. An optimization campaign was then started to explore the SAR around **7** and to improve its pharmacodynamic profile. Compound **7** can be dissected into three main parts: a hydrophobic thiophene moiety connected to the 2-amino-quinoline system through a central linker of basic nature. Interestingly, several groups have previously reported 2-amino-quinoline-containing MCH-R1 antagonists.^{10–15} However, despite the structural similarities, these compounds displayed markedly different SAR when compared to the current chemical series, as detailed below.

Docking¹⁶ of **7** to the homology model of MCH-R1 based on bovine rhodopsin (PDB: 1u19) suggested that the central basic group interacts with D123, a residue involved in the recognition of the MCH peptide.¹⁷ Moreover, the 2-amino-quinoline portion could establish hydrogen bonds with the side chain of Q127, whilst no specific interactions were observed for the thiophene

Keywords: Melanin-concentrating hormone receptor; MCH; MCH-R1 antagonists; Obesity.

* Corresponding authors. Tel.: +46 31 7065723; fax: +46 31 7763710 (F.G.); tel.: +46 31 7761954; fax: +46 31 7763724 (T.I.); e-mail addresses: fabrizio.giordanetto@astrazeneca.com; tord.inghardt@astrazeneca.com

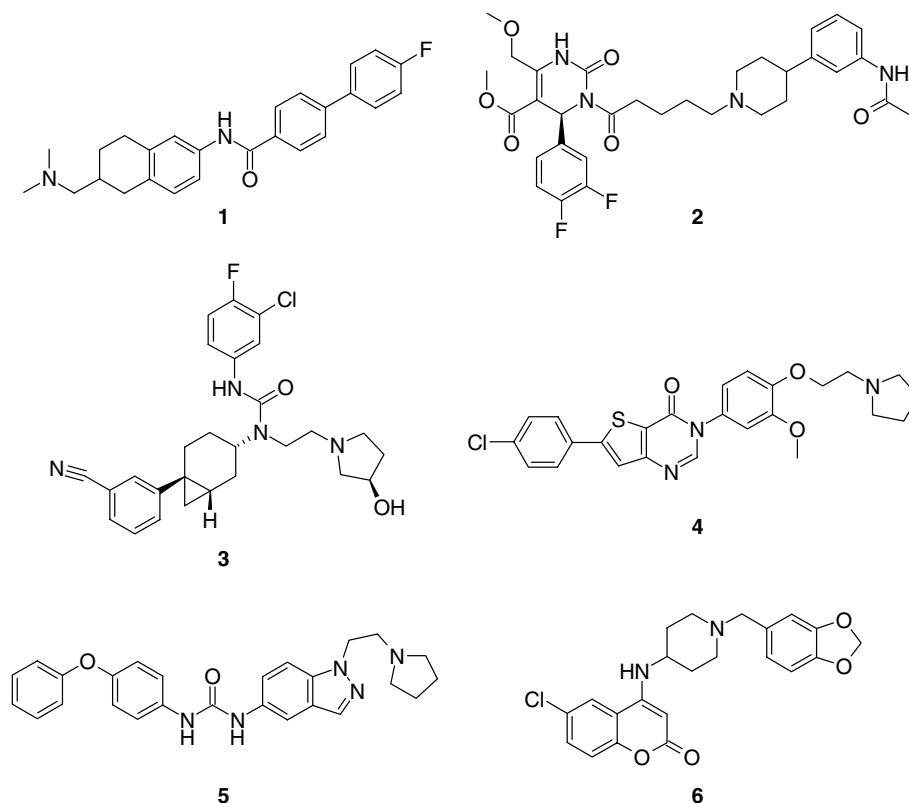


Figure 1. Selected MCH-R1 antagonists.⁹

ring (Fig. 2). Earlier modeling studies highlighted the important role of D123 in the binding of 2-amino-quinoline derivatives.^{14,15} Interestingly, although Q127 is contributing to the binding sites described by Clark et al.,¹⁴ and Ulven et al.,¹⁵ no evident electrostatic interactions with the corresponding ligands have been reported.

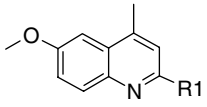
The central linker was the subject of a thorough structural investigation. The purpose was 2-fold: first, to explore its contribution to MCH antagonism and second,

to restrict the conformational degrees of freedom of the initial compound. The flexible nature of the alkyl chain present in **7** could theoretically generate selectivity and polypharmacology issues, considering the ability of a highly flexible ligand to fit into several different binding sites. It was thus felt necessary to identify and lock the bioactive conformation of the lead compound via structural rigidification. The results of such campaign are presented in Table 1.

According to the docked pose, the propane-1,3-diamino moiety of **7** adopts a semi-extended conformation. The ethane-1,2-diamino derivative **8** was prepared to test whether a shorter spacer could mimic the predicted conformation of **7** and to probe the length requirements for the central core. Unfortunately, the smaller alkyl chain ligand (**8**, $IC_{50} = 3.59 \mu M$) resulted in a 239-fold loss of binding affinity over **7**. When docked, **8** is still able to establish a salt bridge with D123. However, although the 2-amino-quinoline system is pointing toward the side chain of Q127, the corresponding distance (3.7 Å) does not permit a hydrogen bond interaction and the pocket surrounding the quinoline ring is only partially filled. These findings could help explain the observed drop in potency. The addition of a carbon atom to yield butane-1,4-diamine (**9**) resulted in a total loss of activity at the tested concentration. There appears to be some specific spatial constraints on the central fragment: these could probably be dictated by the presence of D123 and Q127 on the receptor side. Following such hypothesis, an ideal scaffold would lock the positions of the 2-amino-quinoline group and the secondary amine function



Figure 2. Predicted binding mode of **7** (capped sticks). Polar side chains involved in the binding are rendered as balls-and-sticks.

Table 1. In vitro binding data for a series of central linkers


Compound	R ¹	h-MCH-R1 IC ₅₀ ^a (μM)
7		0.015
8		3.59
9		>33
10		0.003
11		0.411
12		0.062
13		0.035
14		5.01
15		0.369
16		0.106
17		0.119
18		2.99
19		2.30
20		2.13

^a Values are means of at least two experiments. Compounds competed with ¹²⁵I-MCH for binding at the human MCH1 receptor (h-MCH-R1) expressed in the HEK293 cell line.

so as to provide optimal interactions with Q127 and D123, respectively.

A number of cyclic-1,3-diamine analogues (**10–15**) were superimposed onto the docked conformation of **7** to identify potential alternative linkers. According to the results, both cyclohexane and cyclopentane-1,3-diamine derivatives would provide the best three-dimensional alignments to **7**. More specifically, their *trans* configurations (i.e., 1*S*,3*S* or 1*R*,3*R*) would be preferred over the *cis* forms (i.e., 1*S*,3*R* or 1*R*,3*S*). Interestingly, the introduction of (1*S*,3*S*)-cyclohexane-1,3-diamine to afford **10** (IC₅₀ = 3 nM) resulted in an improvement in MCH-R1 binding affinity compared to the simple propane spacer found in **7** (IC₅₀ = 15 nM). It is noteworthy that the opposite enantiomer (1*R*,3*R*) found in **11** showed only moderate MCH-R1 antagonism (IC₅₀ = 411 nM). This may be due to the presence of the cyclohexane ring in a 'forbidden' region of the binding pocket. The docking results suggest that it would face the negatively charged side chain of D123 thus preventing the formation of an optimal salt bridge. Incorporation of (1*S*,3*S*)-cyclopentane-1,3-diamine (**12**) proved to be somehow less favored (IC₅₀ = 62 nM), despite the good alignment to **7** and **10**, and no obvious penalizing interactions in the MCH-R1 binding pocket. In both the cyclohexane and cyclopentane subseries, the *cis* isomers showed a marked decrease in potency (results not shown).

Conformational restriction of the central linker proved to be a successful strategy to gain binding affinity. Assuming a chair conformation as the most populated form of the central scaffold in **10**, there is still the possibility of interconversion between the two different chair forms (i.e., equatorial-axial and axial-equatorial). Introduction of a bicyclo[2.2.1]heptane ring would provide a completely rigid central spacer and could potentially lock the bioactive conformation for these analogues. To our dismay, none of the bicyclo[2.2.1]heptane derivatives synthesized (**13–15**) demonstrated the sought improvement in potency over **10**. The best result was displayed by **13** (IC₅₀ = 35 nM), in which the quinoline ring is in endo of the bridge carbon atom. The bicyclo[2.2.1]heptane structure locks the boat conformation of cyclohexane. If the chair conformation of cyclohexane is indeed the bioactive conformation, then the structural differences between a rigid boat and a flexible chair could be held responsible for the loss of binding affinity. Alternatively, the presence of the additional bridge atom could cause an imperfect fit to the receptor due to the increased steric hindrance of the linker. This second hypothesis seems to be favored by both ligand alignments and docking results. However, according to the computational results, the steric hindrance effect is more evident for both **15** (IC₅₀ = 369 nM) and **14** (IC₅₀ = 5 μM), whereas it is barely noticeable in the case of **7**.

The 2-amino-quinoline and secondary amine functionalities were so far assumed to be essential for potent MCH-R1 antagonism, based on the predicted molecular interactions with the receptor. These hypotheses were challenged in order to gain a better understanding of

the SAR around the MCH-R1 antagonists studied here. Specifically, a pharmacophore model¹⁸ was derived by superimposing the best and most diverse antagonists in the series (**7**, **10**, and **13**), as shown in Figure 3. Three features were defined: the positively charged nitrogen (N⁺) centered on the secondary amine group and two hydrophobic centroids for the thiophene (Hy1) and quinoline (Hy2) rings (Fig. 3). This served as a framework to evaluate molecules in their ability to (1) maintain a good shape similarity to the best compounds and (2) provide alternative structural motifs for the interaction with D123 and Q127. Transformation of the secondary amine functionality of **7** into amide (**16**) afforded a weaker antagonist ($IC_{50} = 106$ nM). Although the amide would still be able to establish a hydrogen bond with D123 through its N–H group, such polar interaction is not preferred and appears to contribute less to the overall binding affinity. This would strengthen the hypothesis that securing a salt bridge with D123 is a key requisite for potency in the current chemical series. However, it cannot be completely ruled out that the observed potency loss originates from other subtle effects such as altered electrostatic properties of the thiophene ring and rigidification of the linker. A number of tertiary amines were also prepared to investigate their effect on binding. Surprisingly, the simple N-methylation of **12** ($IC_{50} = 62$ nM) to provide **17** ($IC_{50} = 119$ nM) translated in a loss of affinity, while inclusion of the piperidine-3-methylamine scaffold (**18**, $IC_{50} = 2.99$ μ M) exhibited a more significant drop in potency.

Modification of the hydrogen bond donor properties of the 2-amino-quinoline moiety was also carried out to verify the supposed interaction with Q127. To this end, compounds lacking a hydrogen bond donor group were prepared, here exemplified by **19** ($IC_{50} = 2.30$ μ M) and **20** ($IC_{50} = 2.13$ μ M), which all displayed poor activity at the receptor. This is in stark contrast with previous reports disclosing 2-amino-quinoline derivatives as MCH-R1 antagonists.^{10–15} These studies clearly demonstrated that tertiary amino-quinolines afforded MCH-R1 antagonists in the low nanomolar range. The differences in binding hypotheses and the role of Q127 may help to rationalize the divergent SAR observed.

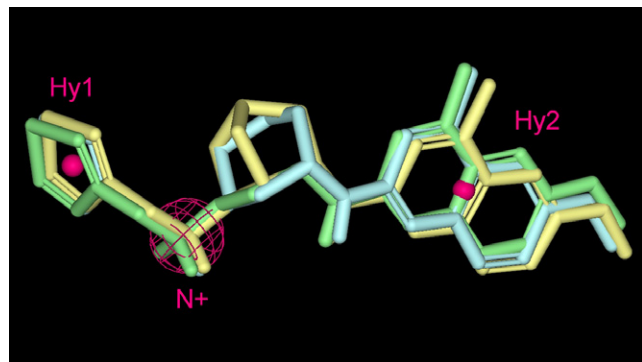
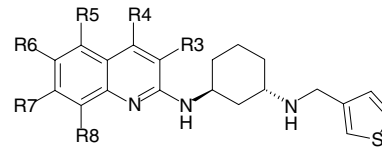


Figure 3. Three-dimensional alignment of **7** (pale green), **10** (light cyan), and **13** (yellow). The pharmacophore features employed in the search for new spacers are also depicted: positive charge (N⁺) and hydrophobic centroids (Hy1 and Hy2).

Although **10** proved to be a very potent MCH-R1 antagonist ($IC_{50} = 3$ nM), its ability to antagonize MCH-R1 signaling in a functional assay (MCH-R1 GTP γ S $IC_{50} = 46$ nM) and its metabolic stability (Human Liver Microsomes intrinsic clearance, HLM $Cl_{int} = 128$ μ L min⁻¹ mg⁻¹) needed to be improved. In this context, both ends of the molecule were metabolized (O-demethylation on the quinoline ring and hydroxylation of the thiophene moiety), whereas the central cyclohexane-diamine scaffold appeared to be stable.

The quinoline system was subjected to a thorough analysis in order to identify the best ring assembly and the corresponding substitution pattern. According to the structure-based modeling results, there appeared to be some room for small modifications in either position 5, 6 or 7 of the quinoline ring. Moreover, position 4 would probably only tolerate very minor replacements, whereas positions 3 and 8 did not seem to allow for any beneficial substitutions. A number of ring alternatives were designed in order to challenge the docking results and to systematically explore the chemical space in that region. These findings are outlined in Table 2. The synthesis of a representative compound, **33**, is outlined in Scheme 1.²⁰ As a first comparison, the unsubstituted quinoline ring of **21** displayed reduced binding and functional activity ($IC_{50} = 68$ nM, GTP γ S $IC_{50} = 234$ nM) when compared to **10**. The 4-methyl-quinoline derivative **22** still maintained potency but showed no improvement in the GTP γ S assay ($IC_{50} = 7$ nM, GTP γ S $IC_{50} = 59$ nM). On the other hand, simplification of **10** to yield the 6-methoxy-quinoline analogue **23** reduced binding but improved functional antagonism ($IC_{50} = 57$ nM, GTP γ S $IC_{50} = 25$ nM), although metabolic stability was not enhanced (HLM $Cl_{int} = 295$ μ L min⁻¹ mg⁻¹). Additional substitutions in position 6 (**24–26**) always translated in a loss of potency, suggesting that the methoxy group is probably optimal. Intriguingly, the potent 2-amino-quinoline-containing MCH-R1 antagonists published by different laboratories displayed an amide function at the 6-position, analogously to **26**, which carried a variety of bulky substituents.^{11–15} The modification of position 4 showed some very interesting results. Replacement of methyl by trifluoromethyl (**27**) or cyano (**28**) drastically reduced binding ($IC_{50} = 4.8$ and 9.9 μ M, respectively). Introduction of dimethylamino maintained activity (**29**, $IC_{50} = 29$ nM, GTP γ S $IC_{50} = 97$ nM), whilst the 4-methoxy-quinoline compound **30** afforded the sought improvement in the functional assay ($IC_{50} = 9$ nM, GTP γ S $IC_{50} = 8$ nM). The observed effects of cyano and dimethylamino substitutions on binding were correctly predicted in silico. However, docking failed to anticipate the loss of potency observed for the trifluoromethyl analogue **27**. A possible explanation may be found in the electron-donating and withdrawing effects that such substitutions exert on the quinoline nitrogen and which are not fully captured by the docking model.

Interestingly, the 4-methoxy-6-fluoro-quinoline derivative (**31**) also resulted in a potent, functional antagonist ($IC_{50} = 26$ nM, GTP γ S $IC_{50} = 9$ nM), whereas the

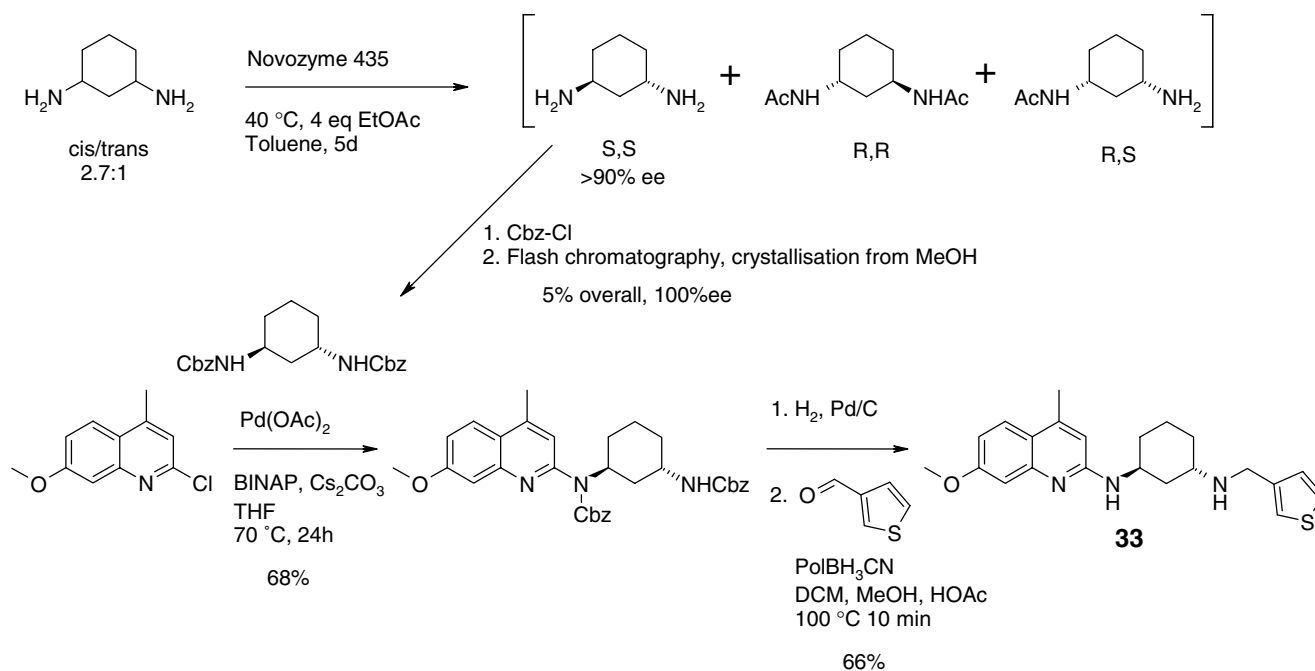
Table 2. In vitro binding and functional data, and HLM intrinsic clearance results for substituted quinolines


Compound	R ³	R ⁴	R ⁵	R ⁶	R ⁷	R ⁸	h-MCH-R1 IC ₅₀ ^a (μM)	h-MCH-R1 GTPγS IC ₅₀ ^b (μM)	HLM Cl _{int} (μL min ⁻¹ mg ⁻¹)
21	H	H	H	H	H	H	0.068	0.234	ND ^c
22	H	Me	H	H	H	H	0.007	0.059	60
23	H	H	H	MeO	H	H	0.057	0.025	295
24	H	H	H	Cl	H	H	0.571	ND ^c	ND ^c
25	H	H	H	Me ₂ N	H	H	0.847	ND ^c	ND ^c
26	H	H	H	AcN(Me)	H	H	2.52	ND ^c	ND ^c
27	H	CF ₃	H	H	H	H	4.8	ND ^c	68
28	H	CN	H	H	H	H	9.92	ND ^c	ND ^c
29	H	Me ₂ N	H	H	H	H	0.029	0.097	30
30	H	MeO	H	H	H	H	0.009	0.008	ND ^c
31	H	MeO	H	F	H	H	0.026	0.09	ND ^c
32	H	MeO	H	<i>i</i> -PrO	H	H	0.231	ND ^c	ND ^c
33	H	Me	H	H	MeO	H	0.0001	0.001	32
34	H	H	MeO	H	H	H	0.054	0.042	38
35	Me	H	H	MeO	H	H	1.39	ND ^c	ND ^c
36	H	H	H	H	H	Cl	5.1	ND ^c	15

^a Values are means of at least two experiments. Compounds competed with [¹²⁵I]-MCH for binding at the human MCH1 receptor (h-MCH-R1) expressed in the HEK293 cell line.

^b Functional assay measuring [³⁵S]GTPγS accumulation.

^c Not determined.

**Scheme 1.**

6-isopropoxy analogue **32** showed a 10-fold drop in binding affinity due to the increased steric bulk and the consequent imperfect fit. A number of 4-methylquinolines were also designed to further investigate the SAR. Notably, the 7-methoxy substituent provided **33**, a very promising MCH-R1 antagonist with excellent binding and functional antagonism abilities

(IC₅₀ = 0.1 nM, GTPγS IC₅₀ = 1 nM). Interestingly, walking the methoxy substituent from the 6- to the 7-position of the quinoline ring significantly improved metabolic stability (HLM Cl_{int} = 32 μL min⁻¹ mg⁻¹) of the MeO-group. The two major metabolites from **33** were hydroxylation at the quinoline ring and a N-dealkylation (cleavage) of the methyl thiophene moiety.

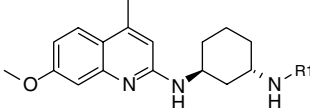
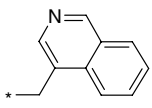
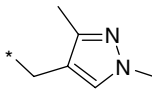
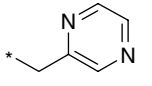
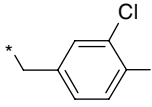
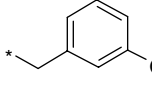
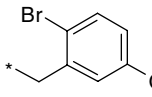
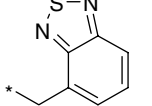
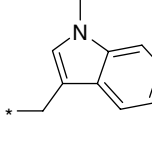
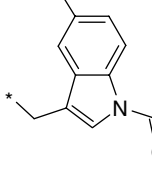
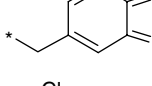
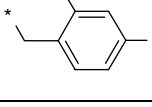
Modifications at positions 3, 5, and 8 to yield **34**, **35**, and **36**, respectively, did not offer any improvement over **33**, as shown in Table 2. The 3-methyl group on **35** forced the quinoline and cyclohexane rings to adopt a conformation that cannot be accommodated in the binding pocket, whilst the 8-chloro substituent of **36** was predicted to spatially impair the hydrogen bond between the quinoline ring and Q127. This is another striking difference in SAR between the current series and other structurally related MCH-R1 antagonists. Specifically, Vasudevan et al. reported 2-amino-8-alkoxy-quinolines as potent MCH-R1 antagonists,¹⁰ suggesting that the two series may adopt different binding modes.

Overall, docking was successful in predicting the consequences of structural changes at the different positions of the quinoline ring. This was especially true for modifications that considerably altered the size and conformation of the ligands. In contrast, subtler variations of their electronic properties, as discussed for the substituents at the 4-position, remained difficult to capture.

The rigidification of the central linker coupled with the optimization of the quinoline ring identified **33**, as a MCH-R1 antagonist with a very promising pharmacodynamic profile. Theoretical concerns around the thiophene moiety, namely the potential to form reactive metabolites,²¹ prompted us to explore safer chemical alternatives. Two libraries were assembled to investigate the effects of thiophene modifications on biological affinity and metabolism. The first library was built around the (1*S*,3*S*)-cyclohexane-1,3-diamine scaffold and designed with the aim to explore the chemical space compatible with the receptor constraints and with drug-like physico-chemical properties.²² Table 3 summarizes the binding data obtained for the library.

Unfortunately, none of the synthesized derivatives displayed an improvement in binding affinity over **10**. The best antagonist was the benzo[1,2,5]thiadiazol-4-yl substituted compound **43** with an IC_{50} value of 10 nM. Interestingly, variation of the substitution pattern on the same ring system to yield **46** resulted in an antagonist of comparable potency (IC_{50} = 16 nM). Introduction of other fused heterocycles comprising isoquinoline (**37**: IC_{50} = 22 nM) and substituted indoles (**44**, **45**: IC_{50} 's = 61 and 58 nM, respectively) did not improve potency. Moreover, installing single ring, heteroaryl moieties, exemplified by pyrazine **39** (IC_{50} = 89 nM) and 1,3-dimethyl-pyrazole **38** (IC_{50} = 178 nM), proved detrimental for potency. These findings suggest that polarized ring systems are not very well tolerated. This could be due to the fact that the binding pocket has mainly a lipophilic character, and burial of polar moieties would be energetically unfavored. Among the phenyl-substituted analogues, 3,4-dichloro-phenyl and 3-trifluoromethoxy-phenyl afforded the best compounds (**40**, IC_{50} = 13 nM and **41**, 15 nM), whereas the 2-bromo-5-methoxy-phenyl derivative **42** (IC_{50} = 28 nM) and the 2-chloro-4-methanesulfonyl-phenyl analogue **47** (IC_{50} = 50 nM) displayed a potency loss when compared to **10**. Regrettably, none of the compounds in the cyclohexane library displayed an improved meta-

Table 3. In vitro binding functional affinity and HLM intrinsic clearance data for **37–47**

			
Compound	R ¹	h-MCHr1 IC_{50}^a (μM)	HLM Cl_{int} (μL min ⁻¹ mg ⁻¹)
37		0.022	500
38		0.178	ND ^b
39		0.089	ND ^b
40		0.013	59
41		0.015	64
42		0.028	ND ^b
43		0.010	ND ^b
44		0.061	41
45		0.058	52
46		0.016	227
47		0.050	269

^a Values are means of at least two experiments. Compounds competed with [¹²⁵I]-MCH for binding at the human MCH1 receptor (h-MCH-R1) expressed in the HEK293 cell line.

^b Not determined.

Table 4. In vitro binding and functional affinities, and HLM intrinsic clearance data for **48–55**

Compound	R ¹	h-MCH-R1 IC ₅₀ ^a (μM)	h-MCH-R1 GTPγS IC ₅₀ ^b (μM)	HLM Cl _{int} (μL min ⁻¹ mg ⁻¹)
48		0.009	0.085	<12
49		0.005	0.035	12
50		0.080	ND ^c	26
51		0.029	0.083	20
52		0.071	ND ^c	12
53		0.033	0.118	<12
54		0.020	0.127	<12
55		0.039	ND ^c	<12

^a Values are means of two experiments. Compounds competed with ¹²⁵I-MCH for binding at the human MCH1 receptor (h-MCH-R1) expressed in the HEK293 cell line.

^b Functional assay measuring [³⁵S]GTPγS accumulation.

^c Not determined.

bolic profile over **10**. Here, compound **44** was the most stable, with a HLM Cl_{int} of $41 \mu\text{L min}^{-1} \text{mg}^{-1}$.

The second library used the (1*S*,3*S*)-cyclopentane-1,3-diamine, which is synthetically more easily accessible²³ when compared to the cyclohexane analogue. Additionally, we observed that cyclopentane derivatives had in general improved metabolic stability over cyclohexane compounds (cf **10** and **12**, HLM Cl_{int} = 128 and $78 \mu\text{L min}^{-1} \text{mg}^{-1}$, respectively). For this library, we adopted a more focused design around the indole ring of **48**, which showed good potency and low intrinsic clearance in human liver microsomes, as outlined in Table 4. The synthesis of compound **51** is shown in Scheme 2.²⁰

Overall the library was successful in identifying metabolically stable compounds. However, coupling stability with potency in the low, single-digit nanomolar range proved more difficult. Substitutions on position 5 of the indole ring greatly affected the binding ability of the compounds. 5-Difluoromethoxy afforded the best antagonist in the library, **49**, with an IC_{50} value of 5 nM and an intrinsic HLM clearance value of 12. Interestingly, the 5-benzyloxy-group on **50** compromised potency (IC_{50} = 80 nM), corroborating the finding that there are steric constraints in the receptor pocket. More importantly, the introduction of a cyano group on the indole (**53–55**) always resulted in very stable antagonists with HLM clearance values of less than 12, thereby highlighting the importance of reducing the electron density on the ring as a means of diminishing oxidative metabolism.

Following the positive pharmacodynamic and metabolic stability results (Table 4), compounds **49** and **51** were evaluated in a diet-induced obesity (DIO) model in

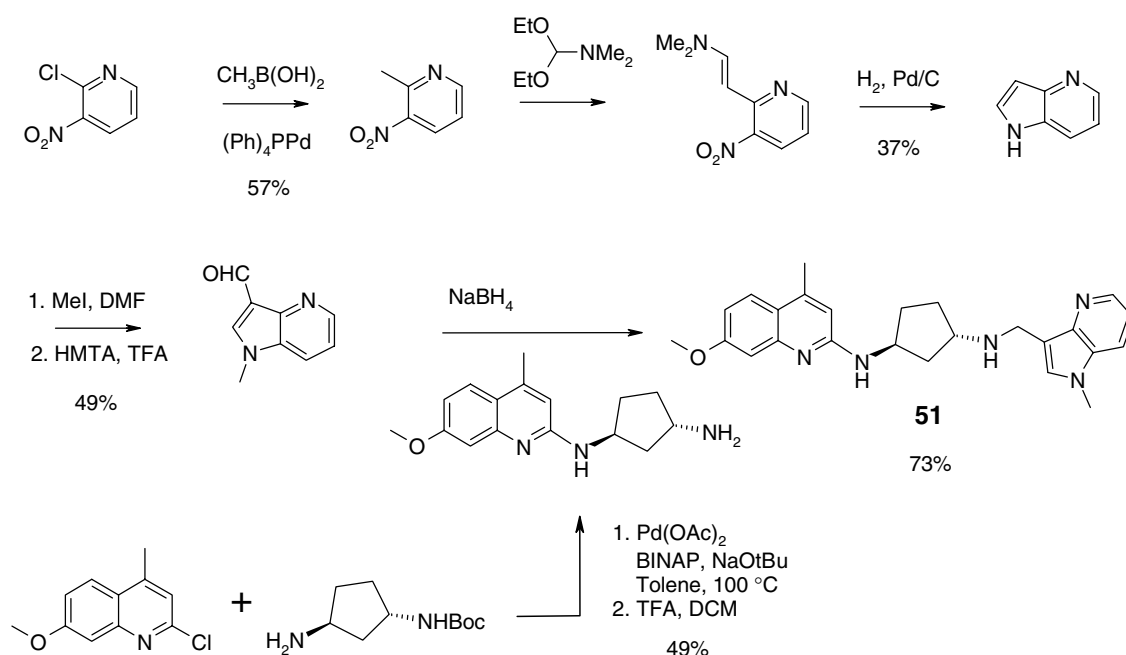
mouse,²⁴ to assess their effects on food intake and weight reduction. Animals were dosed perorally for 5 days with a daily dose of 20 and 50 $\mu\text{mol/kg}$, respectively. Disappointingly, we could not observe any statistically significant body weight reduction in these experiments. We then examined the pharmacokinetic (PK) characteristics of the compounds in order to investigate and rationalize their lack of in vivo efficacy. The PK profile of compound **51** in lean mice is shown in Table 5. Despite showing excellent oral bioavailability, compound **51** gave only a modest brain exposure (Brain/Plasma C_{max} ratio = 0.13, brain C_{max} = 500 nmol/kg). Additionally, plasma protein binding for compound **51** is high (f_u = 6.5% in mouse plasma) and this indicates a high degree of protein and/or tissue binding in the brain.²⁵ We therefore speculate that the lack of efficacy in obese mice can be attributed to an insufficient occupancy of the MCH receptor.²⁶

In summary, optimization of the initial lead compound **7** led to the discovery of several highly potent MCH-R1 antagonists. Structural rigidification of the central

Table 5. Mouse in vivo pharmacokinetic profile of **51**

Parameter ^a	Value
CL (mL/min*kg)	15
V_{ss} (L/kg)	7.6
Fpo (%)	100
$t_{1/2}$ (h) plasma	8.6
C_{max} brain ($\mu\text{mol/kg}$)	0.5
T_{max} brain (h)	0.26
C_{max} plasma ($\mu\text{mol/L}$)	3.78
T_{max} plasma (h)	24
C_{max} brain/ C_{max} plasma	0.13

^a Determined following oral and iv administration of a 20 $\mu\text{mol/kg}$ nanosuspension dose in C57BL female mice.



Scheme 2.

diamine spacer identified (1*S*,3*S*)-cyclohexane-1,3-diamine and (1*S*,3*S*)-cyclopentane-1,3-diamine as the best scaffolds. Subsequent optimization of the substitution pattern on the quinoline ring afforded **33** (IC₅₀ = 0.1 nM, GTPγS IC₅₀ = 1 nM), the most active MCH-R1 antagonist in the present study. Systematic structural exploration aimed at replacing thiophene identified **51** as a novel, potent, and metabolically stable MCH-R1 antagonist. Unfortunately, lack of efficacy in the DIO model, at therapeutically meaningful doses, precluded advancement of any member of this lead series into further development.

Acknowledgments

The authors thank their AstraZeneca coworkers Mia Boethius-Litzén, Susanne Ekehed, Mikael Rehngren, and Arja Schedwin for providing MCH-R1 binding and functional data, human CLint data, and in vivo PK data, respectively, as well as Pernilla Håkansson for running the mouse diet-induced obesity model.

References and notes

- Bittencourt, J. C.; Presse, F.; Arias, C.; Peto, C.; Vaughan, J.; Nahon, J. L.; Vale, W.; Sawchenko, P. E. *J. Comp. Neurol.* **1992**, *319*, 218.
- Skofitsch, G.; Jacobowitz, D. M.; Zamir, N. *Brain Res. Bull.* **1985**, *15*, 635.
- Saito, Y.; Nothacker, H.-P.; Civelli, O. *Trends Endocrinol. Metab.* **2000**, *11*, 299.
- Schwartz, M. W.; Woods, S. C.; Porte, D.; Selley, R. J.; Baskin, D. G. *Nature* **2000**, *404*, 661.
- Qu, D.; Ludwig, D. S.; Grammeltoft, S.; Piper, M.; Pellemounter, M. A.; Cullen, M. J.; Mathes, F. W.; Przypek, J.; Kanerek, R.; Maratos-Flier, E. *Nature* **1996**, *380*, 243.
- Gomori, A.; Ishiara, A.; Ito, M.; Mashiko, S.; Matsuhita, H.; Yumoto, M.; Ito, M.; Tanaka, T.; Tokita, S.; Moriya, M.; Iwaasa, H.; Kanatani, A. *Am. J. Physiol. Endocrinol. Metab.* **2003**, *284*, E583.
- Ludwig, D. S.; Tritos, N. A.; Mastaitis, J. W.; Kulkarni, R.; Kokkotou, E.; Elmquist, J.; Lowell, B.; Flier, J. S.; Maratos-Flier, E. *J. Clin. Invest.* **2001**, *107*, 379.
- Shimada, M.; Tritos, N. A.; Lowell, B. A.; Flier, J. S.; Maratos-Flier, E. *Nature* **1998**, *396*, 670.
- (a) Takekawa, S.; Asami, A.; Ishihara, Y.; Terauchi, J.; Kato, K.; Shimomura, Y.; Mori, M.; Murakoshi, H.; Suzuki, N.; Nishimura, O.; Fujino, M. *Eur. J. Pharmacol.* **2002**, *438*, 129; (b) Borowsky, B.; Durkin, M. M.; Ogozalek, K.; Marzabadi, M. R.; DeLeon, J.; Lagu, B.; Heurich, R.; Lichtblau, H.; Shaposhnik, Z.; Daniewska, I., et al. *Nat. Med.* **2002**, *8*, 825; (c) McBriar, M. D.; Guzik, H.; Xu, R.; Paruchova, J.; Li, S.; Palani, A.; Clader, J. W.; Greenlee, W. J.; Hawes, B. E.; Kowalski, T. J.; O'Neill, K., et al. *J. Med. Chem.* **2005**, *48*, 2274; (d) Handlon, A. L.; Al-Barazanji, K. A.; Barvian, K. K.; Bighan, E. C.; Carlton, D. L.; Carpenter, A. J.; Cooper, J. P.; Daniels, A. J.; Garrison, D. T.; Goetz, A. S., et al. 228th American Chemical Society National Meeting, Philadelphia, PA, USA, 2004: MEDI-193; (e) Iyengar, R.; Souers, A. J.; Lynch, J. K.; Judd, A. S.; Gao, J.; Freeman, J. C.; Mulhern, M.; Vasudevan, A.; Wodka, D.; Blackburn, C., et al. 230th American Chemical Society National Meeting, Washington, DC, USA, 2005: MEDI-086; (f) Souers, A. J.; Gao, J.; Wodka, D.; Judd, A. S.; Mulhern, M. M.; Napier, J. J.; Brune, M. E.; Bush, E. N.; Brodjian, S. J.; Dayton, B. D.; Shapiro, R.; Hernandez, L. E.; Marsh, K. C.; Sham, H. L.; Collins, C. A.; Kym, P. R. *Bioorg. Med. Chem. Lett.* **2005**, *15*, 2752.
- Vasudevan, A.; Wodka, D.; Verzal, M. K.; Souers, A. J.; Gao, J.; Brodjian, S.; Fry, D.; Dayton, B.; Marsh, K. C.; Hernandez, L. E.; Ogiela, C. A.; Collins, C. A.; Kym, P. R. *Bioorg. Med. Chem. Lett.* **2004**, *14*, 4879.
- Arienzo, R.; Clark, D. E.; Cramp, S.; Daly, S.; Dyke, H. J.; Lockey, P.; Norman, D.; Roach, A. G.; Stuttle, K.; Tomlinson, M.; Wong, M.; Wren, S. P. *Bioorg. Med. Chem. Lett.* **2004**, *14*, 4099.
- Ulven, T.; Little, P. B.; Receveur, J.; Frimurer, T. M.; Rist, Ø.; Nørregaard, P. K.; Högberg, T. *Bioorg. Med. Chem. Lett.* **2006**, *16*, 1070.
- Jiang, J.; Hoang, M.; Young, J. R.; Chaung, D.; Eid, R.; Turner, C.; Lin, P.; Tong, X.; Wang, J.; Tan, C., et al. *Bioorg. Med. Chem. Lett.* **2006**, *16*, 5270.
- Clark, D. E.; Higgs, C.; Wren, S. P.; Dyke, H. J.; Wong, M.; Norman, D.; Lockey, P. M.; Roach, A. G. *J. Med. Chem.* **2004**, *47*, 3962.
- Ulven, T.; Frimurer, T. M.; Receveur, J.; Little, P. B.; Rist, Ø.; Nørregaard, P. K.; Högberg, T. *J. Med. Chem.* **2005**, *48*, 5684.
- Giordanetto, F.; Lindberg, J.; Karlsson, O.; Inghardt, T. *Abstract of Papers*, 232nd National Meeting of the American Chemical Society, San Francisco, CA, 2006, COMP-410.
- Macdonald, D.; Murgolo, N.; Zhang, R.; Durkin, J. P.; Yao, X.; Strader, C. D.; Graziano, M. P. *Mol. Pharmacol.* **2000**, *58*, 217.
- Three-dimensional alignments were carried out with ROCS (OpenEye Scientific Software, 3600 Cerrillos Rd., Suite 1107, Santa Fe, NM 87507) using the Shape Tanimoto function to quantify similarity. An in-house pharmacophore search method¹⁹ was employed to identify central linkers that satisfied the three pharmacophoric features described (N+, Hy1, and Hy2) within a root mean square deviation of 0.75 Å.
- Lyne, P. D.; Kenny, P. W.; Cosgrove, D. A.; Deng, C.; Zabudoff, S.; Wendoloski, J. J.; Ashwell, S. *J. Med. Chem.* **2004**, *47*, 1962.
- The preparation of representative compounds is described in: Ray, A. K.; Sigfridsson, E. M.; Linusson, A.; Stina, M.; Sandberg, P. M.; Inghardt, T.; Svensson, A. M.; Brickmann, K. WO2004/004726 (compound **9**), and in: Evertsson, E.; Inghardt, T.; Lindberg, J.; Linusson, A.; Giordanetto, F. WO2005/066132 (compounds **13**, **15**, **23**, **29**, **31**, **38**, **41**, **43**, **49–55**).
- Dansette, P. M.; Thang, D. C.; El Amri, H.; Mansuy, D. *Biochem. Biophys. Res. Commun.* **1992**, *186*, 1624.
- A variety of structural descriptors, including log *D* and aqueous solubility predictions, served to profile and filter the chemical library. These were calculated using in-house developed models implemented in Pipeline Pilot version 4.5, SciTegic: San Diego, CA.
- The preparation of *tert*-butyl[(1*S*,3*S*)-3-aminocyclopentyl]carbamate is detailed in Evertsson, E.; Inghardt, T.; Lindberg, J.; Linusson, A.; Giordanetto, F. WO2005/066132.
- Female C57Bl/6J mice were given ad libitum access to calorie-dense 'cafeteria' diet (soft chocolate/cocoa-type pastry, chocolate, fatty cheese, and nougat) and standard lab chow for 8–10 weeks until a body weight of 45–50 g was achieved. Compounds to be tested were then admin-

istered perorally once daily for a period of 5–12 days, and the body weights of the mice monitored on a daily basis. During this period ad libitum access to calorie-dense ‘cafeteria’ diet and standard lab chow was maintained.

25. Wan, H.; Rehngren, M.; Giordanetto, F.; Bergström, F.; Tunek, A., *J. Med. Chem.*, submitted for publication.
26. Maurer, T. S.; DeBartolo, D.; Tess, D. A.; Scott, D. O. *Drug Metab. Dispos.* **2005**, 33, 175.